

SeaTurtleID: A novel long-span dataset highlighting the importance of timestamps in wildlife re-identification

Kostas Papafitsoros
School of Mathematical Sciences
Queen Mary University of London
Mile End Road, E1 4NS, UK
k.papafitsoros@qmul.ac.uk

Vojtěch Čermák
Faculty of Electrical Engineering
Czech Technical University in Prague
Technická 2, 166 27, Prague, Czechia
cermavo3@fel.cvut.cz

Lukáš Adam
Faculty of Electrical Engineering
Czech Technical University in Prague
Technická 2, 166 27, Prague, Czechia
adamluk3@fel.cvut.cz

Lukáš Pícek
Faculty of Applied Sciences
University of West Bohemia
Technická 8, 301 00, Plzeň, Czechia
picekl@kky.zcu.cz

Abstract

This paper introduces SeaTurtleID, the first public large-scale, long-span dataset with sea turtle photographs captured in the wild. The dataset is suitable for benchmarking re-identification methods and evaluating several other computer vision tasks. The dataset consists of 7774 high-resolution photographs of 400 unique individuals collected within 12 years in 1081 encounters. Each photograph is accompanied by rich metadata, e.g., identity label, head segmentation mask, and encounter timestamp. The 12-year span of the dataset makes it the longest-spanned public wild animal dataset with timestamps. By exploiting this unique property, we show that timestamps are necessary for an unbiased evaluation of animal re-identification methods because they allow time-aware splits of the dataset into reference and query sets. We show that time-unaware (random) splits can lead to performance overestimation of more than 100% compared to the time-aware splits for both feature- and CNN-based re-identification methods. We also argue that time-aware splits correspond to more realistic re-identification pipelines than the time-unaware ones. We recommend that animal re-identification methods should only be tested on datasets with timestamps using time-aware splits, and we encourage dataset curators to include such information in the associated metadata.

1. Introduction

Image-based individual animal re-identification, that is, the process of recognising individual animals based on their

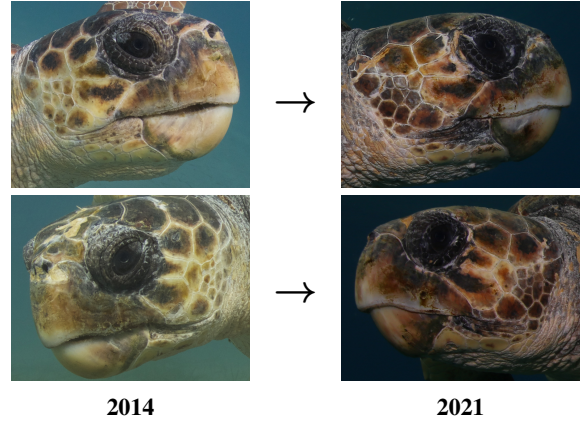


Figure 1: Different visual appearance of the same individual sea turtle over 7 years due to different *factors* like camera capture conditions and animal ageing. The shapes of the facial scales remained stable, but other features have changed over time, like colouration, pigmentation, shape, and scratches.

unique stable-over-time external characteristics, is an essential tool for studying different aspects of wildlife, like population monitoring, movements, behavioural studies, and wildlife management [41, 50, 35, 44]. The increasing sizes of the associated photo databases stemming from the multi-year span of such projects [46, 43] have highlighted the need for automated methods to reduce the labour-intensive human supervision in individual animal identification.

As a result, a plethora of automatic re-identification methods have been developed during the last years [13, 6,

51, 31, 22]. Evaluation of these methods is performed on benchmark databases, covering several animal groups like mammals [48, 49, 32, 24, 1, 55], reptiles [2, 17], and smaller organisms [18, 7, 40]. Typically such databases are split into a *reference set* – a set of images with individuals whose identity (label) is known and a *query set* – the set of images with individuals whose identity needs to be matched to the reference set. For deep learning methods, these are described as the training and the testing set, respectively.

The quality of datasets influences the objectivity of the method evaluation, i.e., the photographs in the dataset should mimic a realistic re-identification scenario, in which the images in the query set (corresponding to newly obtained images) are captured under different *factors* than the ones in the reference set. Here by factors, we mean changes in the surrounding environment (e.g. water depth, occlusion, light conditions), image capture conditions (e.g. camera type, flash, type of lenses), but also changes to the individual animals (e.g. due to ageing or injuries). Fig. 1 shows an example of such changes to an individual animal over a long period.

Typically multiple images produced during one *encounter* (burst mode in camera traps, consecutive video frames, multiple photographs taken during an animal-human encounter) share the same factors as the encounter lasts for a short period. The most efficient way to indicate different encounters and hence different factors in a dataset is by including the capture date and time, i.e., *timestamps*, in metadata.

Without timestamps, datasets can be split into reference and query sets only randomly. Thus, images in reference and query sets might share similar factors, and methods for animal re-identification may focus on factors of a particular encounter instead of learning an inner representation of each individual. Therefore, random splits are expected to lead to an overestimation of the generalisation ability of the methods to recognise individuals in future encounters. In other words, a random split implicitly assumes that one will encounter the same factors in the future, which is highly unrealistic. On the other hand, timestamps allow for time-aware splits, where images from a time period are all in either the reference or the query set. This leads to a more realistic case when new factors are encountered in the future. Moreover, if an animal dataset has a long enough time span (difference of last and first date), it allows investigating ageing individuals, a crucial aspect for long-living species.

The survey in [3] showed that from 30 public animal datasets only 5 contain timestamps; see Table 1. From those, Cows2021 and GiraffeZebraID span only one month, and WhaleSharkID includes timestamps for only 9% of photographs. This leaves only two wildlife datasets with timestamps that, however, have a span of at most two years.

To address this gap, we introduce a novel dataset with

photographs of loggerhead sea turtles (*Caretta caretta*) – the *SeaTurtleID*. The dataset was collected over 12 years, and it consists of 7774 high-resolution photographs of 400 unique individuals, all containing timestamps. For the sake of reproducibility and with the aspiration to make it a benchmark dataset for evaluating and comparing automated re-identification algorithms, we make our dataset publicly available.¹ We also accompany it with timestamps, full annotations, labelling bounding boxes and segmentation masks of the unique identifying features of the animals (facial polygonal scales). To our best knowledge, this is the longest-spanned public wild animal dataset for which timestamps are provided and the only public dataset of sea turtles with photographs captured in the wild. We also stress that this dataset is actively expanded on a yearly basis, and a plethora of ecological studies have been based on it [43, 45, 36, 44, 34, 33, 35].

By taking advantage of the long span and the timestamp information of our dataset, we split it into reference and query sets in both time-aware and time-unaware (random) fashion. We proceed by testing two re-identification methods (a feature- and a CNN-based one) and show that time-unaware splits can lead to the overestimation of the capabilities of the methods by more than 100% compared to time-aware splits. Hence, we recommend that developers should only evaluate re-identification algorithms in datasets containing timestamps, employing time-aware splits. Additionally, imaging data collectors and database curators should ensure that time information is included in the metadata.

Even though the main focus here is animal re-identification and properly evaluating associated algorithms by using the timestamps, the SeaTurtleID dataset can be used for the evaluation and testing of several fundamental problems including: (i) object detection, (ii) semantic segmentation, (iii) weakly supervised semantic segmentation, (iv) 3D reconstruction, and (v) concept drift analysis.

¹www.kaggle.com/wildlifedatasets/SeaTurtleID

Dataset	n _{image}	n _{time}	n _{indiv}	n _{enc}	span
BelugaID [1]	5902	100%	788	1241	785
Cows2021 [19]	8670	100%	181	3036	31
GiraffeZebraID [37]	6925	100%	2051	2494	12
MacaqueFaces [53]	6280	100%	34	494	525
WhaleSharkID [21]	7693	9%	98	424	1971
SeaTurtleID (ours)	7774	100%	400	1081	4092

Table 1: All publicly available animal re-identification datasets with timestamps. The columns show the number of photographs, percentage of photographs with timestamps, number of individuals, number of encounters and dataset span in days.

We stress that SeaTurtleID lacks common drawbacks of other (human) re-identification datasets. In particular, face identification datasets typically contain racial bias, the photographs have low resolution, are restricted to limited poses, have limited time spans and are either artificially generated [4], or collected by crawling the internet [23], raising privacy concerns.

We summarise the major contributions of our paper:

- We provide the high-quality dataset – SeaTurtleID – the first large-scale dataset for sea turtle identification in the wild containing 7774 photographs of the 400 individual turtles collected over 12 years (2010–2021). We provide metadata for every photograph, namely identity labels, head orientation labels, head segmentation masks and bounding boxes.
- Crucially, for re-identification benchmarking, we provide a timestamp for every photograph.
- We provide empirical evidence that a time-unaware split of the dataset into reference and query sets leads to a significant overestimation bias compared to a bias-corrected time-aware split approach. Thus, we argue that database curators should include timestamps in metadata.

2. New dataset: SeaTurtleID

This section explains the data collection process and describes key features of the presented dataset and annotation procedures.

2.1. Data collection

Location and species All photographs were taken in Laganas Bay, Zakynthos Island, Greece (37°43'N, 20°52'E), from 2010 until 2021; May-October. Laganas Bay is a main breeding site for the Mediterranean loggerhead sea turtles [30]. Female turtles (around 300 annually) are mainly migratory and visit the island to breed every 2–3 years [43]. On the other hand, certain individuals reside on the island, and they can be observed in consecutive years [35, 44]. Loggerheads are long-lived species, and they can have reproductive longevity of more than three decades [29], which can lead to long-span image recordings for specific individuals. Sea turtles are particularly amenable to photo-identification due to their scale patterns [42]. In particular, the polygonal scales in the lateral (side) and dorsal (top) sides of their heads are unique to every individual and remain stable throughout their lives [10], see Fig. 1 and additional examples in the supplementary material. Notably, the left and right side patterns differ for a given turtle.

Photographic procedure All photographs were captured underwater during snorkelling surveys from a distance ranging from 7 metres to a few centimetres using

three cameras: (i) Canon IXUS 105 digital compact camera with a Canon underwater housing in 2010–2013, (ii) Canon 6D full-frame DSLR camera combined with a Sigma 15mm fisheye lenses and an Ikelite underwater housing in 2014–2017, and (iii) the same camera with an additional INON Z330 external flash in 2018–2021. The resolution ranges from 4000×3000 (Canon IXUS) to 5472×3648 pixels (Canon 6D) with an average of 5289×3546 . The water depth ranged from 1 to 8 metres, with the vast majority of photographs taken less than 5 metres deep.

Photographs taken in 2014–2021 are generally of better quality due to the use of a more advanced camera and a shorter camera-subject distance. On the other hand, due to the use of fisheye lenses, barrel shape distortion can be noticeable, especially for close-up photographs. Finally, more natural colours were acquired using the external flash. In Fig. 2, we display three images of the same individual – obtained by the three different camera set-ups – to highlight the resulting visual differences.

2.2. Dataset highlights

Large-scale in the wild dataset With 7774 photographs and 400 individuals, the dataset represents the most extensive publicly available dataset for sea turtle identification in the wild. The images are uncropped and with various backgrounds. Approximately 90% of photographs have size 5472×3648 pixels, the average photograph size is 5289×3546 pixels, while the head occupies on average 639×551 pixels. Fig. 3 shows the number of photographs for each individual. The majority (239/400) of individuals have at least ten photographs (depicted by the dashed line). Similarly, most individuals (228/400) were encountered at least twice. We note that this number is expected to increase in the following years since this dataset is updated annually.

Long time span & timestamps The dataset contains photographs continuously captured over 12 years from 2010 to 2021. In contrast to most existing animal datasets that are usually collected in controlled environments and/or over a short time span, the SeaTurtleID dataset includes a timestamp (date in day/month/year format) for each photograph.

Fig. 4 (left) shows the number of encounters for each year, with a significantly larger number from 2015 onwards. We note that this is driven by an increasing data collection effort rather than reflecting actual annual animal abundance. Furthermore, Fig. 4 (middle) and (right) show the distribution of the 400 individuals with respect to the total number of observation years and the total span in years. A span of one year means that a turtle was photographed only in one year. Many turtles (166/400) were photographed in at least two different years, and three turtles spanned ten years.

Segmentation masks and bounding boxes Almost all photographs in the dataset (7582/7774) have a clearly visi-



Figure 2: Individual “t023” in the SeaTurtleID database, photographed with three different camera set-ups. Photographs taken with the DSLR camera are of higher quality, and the additional use of flash recovers the natural colouration of the animal. All the photographs were cropped for illustration purposes.

ble head. For these photographs, we annotated the bounding box, the segmentation mask of the head, and the head orientation (left, right, top, top-right, top-left, front, bottom). We provide details for the annotation procedure in the next section. Such annotations allow additionally the evaluation of novel methods for object detection and supervised or weakly semantic segmentation.

Multiple poses The dataset includes multiple images from different angles and, therefore, provides a ground for the challenging task of 3D animal reconstruction.

Summary We summarise all the above information in Tab. 2. For perspective, we also compare SeaTurtleID with the ZindiTurtleRecall dataset [2], which is the only other publicly available sea turtle dataset [3]. We stress that the latter dataset contains photographs in a controlled environment (a rehabilitation centre) with no timestamps.

2.3. Data annotation procedure

Annotation of individual identities The database curator – experienced in sea turtle identification – annotated all the images with individual turtle identities before this work. This annotation was validated by the automatic re-

identification methods described in the next section.

Annotation of head segmentation masks To generate the head segmentation masks and the corresponding bounding boxes, we used a combination of manual and machine-run annotation procedures. We provide a short description here and more details in the supplementary material. We used the [Computer Vision Annotation Tool](#) to manually annotate heads in 1000 photographs and used these masks as training data for four segmentation models. The trained models were used to predict segmentation masks on the whole dataset. We considered a prediction correct when at least three out of four models agreed on it. We manually verified these predictions and retrained the four networks. This process was repeated in five rounds, after which we manually labelled the remaining photographs. We summarise this procedure in Tab. 3. The first row shows the number of new predictions in which at least three of four models agreed on the predictions. The second row then

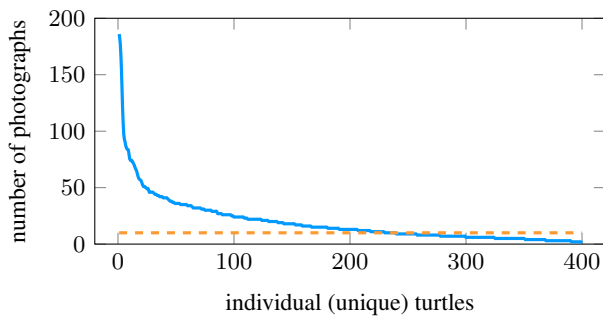


Figure 3: Number of photographs for each of the 400 turtles. The orange line corresponds to 10 photographs.

	SeaTurtleID	ZindiTurtleRecall
Sea turtle species	Loggerheads	Greens/Hawksbills
Images	7774	12803
Individuals	400	2265
Image average size	5289×3546	1382×1118
Head average size	639×551	1382×1118
Location	underwater	land (rehab. centre)
Wild	✓	✗
Not cropped	✓	✗
Timestamp	✓	✗
Head bounding box	✓	✓
Head segmentation	✓	✗
Head orientation	✓	partially

Table 2: SeaTurtleID dataset statistics and direct comparison with the ZindiTurtleRecall dataset [2].

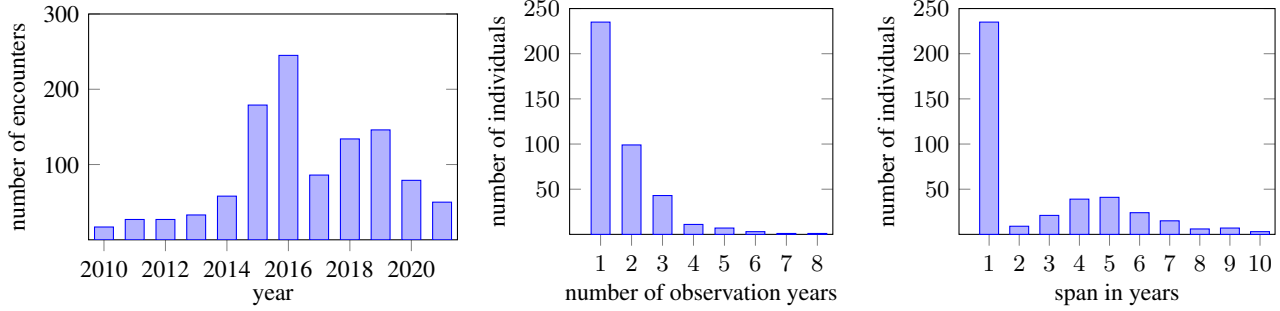


Figure 4: Timestamp information about the SeaTurtleID dataset: number of encounters per year (left), distribution of all individuals with respect to the total number of observation years (middle) and with respect to the total span in years (right).

	Round 1	Round 2	Round 3	Round 4	Round 5	Manual
New predictions	4420	1333	438	818	541	506
New verified predictions	4402	1287	398	769	412	506
Total verified predictions	4402	5689	6087	6856	7268	7774
Remaining	3372	2085	1687	918	506	0

Table 3: Summary of the head segmentation procedure by combining manual and automatic pipelines. After initially labelling 1000 photographs, we run five rounds of an automatic segmentation mask generation (with manual verification), with the last round purely manual. This procedure reduced the manual annotation effort from 7774 to 1506 photographs.

shows the verified (correct) predictions. Since these two numbers are almost identical, the models were mostly correct in their predictions. The last two lines show the total number of verified predictions and the remaining number of photographs to be labelled. In summary, we reduced the manual annotation effort from 7774 to 1506 photographs (1000 originally labelled and 506 labelled in the last manual round), and we obtained a trained model which can be used to obtain segmentation masks of future images.

Annotation of head orientations Since this process is not time-consuming, we did not automatise it but wrote a simple application which loaded each photograph and offered one of the possible orientations for the user to choose.

3. Re-identification methodology

We describe here how we numerically verified our main hypothesis, i.e., that time-aware splits of the database into reference and query sets correct overestimation biases in evaluating algorithms for animal re-identification. Such algorithms can be roughly divided into two families, namely feature-based and neural network-based methods. Feature-based methods typically use techniques from computer vision, e.g., SIFT [28], SURF [5], and ORB [38], to compare the degree of similarities between the salient morphological characteristics of animals. Deep learning-based methods exploit the wide availability of animal images to train deep neural network classifiers [11]. For our purposes, we em-

ploy two re-identification algorithms, one from each family.

3.1. Feature-based method

This method consists of two steps. The first step is based on extracting SIFT features from images similar to Hotspotter [13], combined with a feature alignment check via a projective transform; see more details in the supplementary material. This step decides whether each pair of images contains the same individual. The step is configured so that

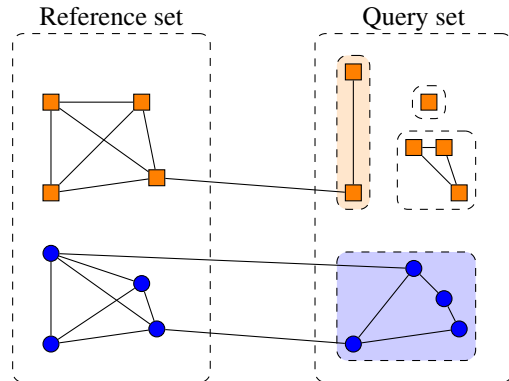


Figure 5: Feature-based method: Connecting edges corresponds to the method’s prediction that the images contain the same turtle. It predicted 4 “blue” turtles, 2 “orange” turtles and gave no prediction for 4 turtles in the query set.

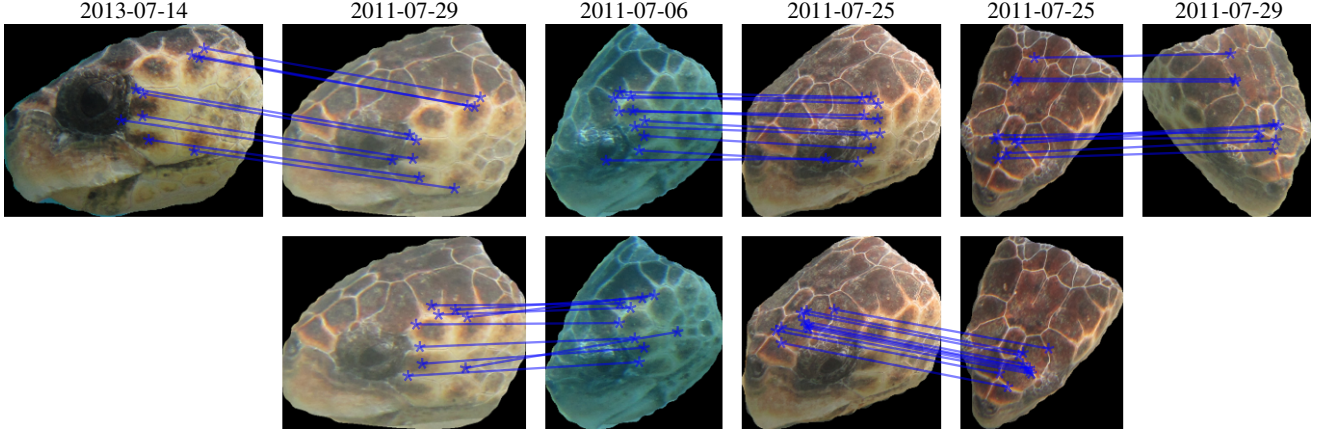


Figure 6: Successively matching the left and right profiles of an individual turtle via images that contain poses of intermediate orientations. Each matching is based on the feature-based method described in Section 3.1. The timestamps (dates) for every image are provided at the top.

it is acceptable not to match two images with the same individual (false negatives are accepted) while avoiding matching two images with different individuals (false positives are minimised).

The second step creates a graph, where nodes are images and edges are matches from the first step. An image from the query set is given a prediction (an identity) if it is connected to an image in the reference set. Moreover, a match can also be achieved if a second query image is connected to the first one, which is connected to an image in the reference set. If the query image is not matched with any images in the reference set, either directly or via another query image, then no prediction is made. We provide an example in Fig. 5. There, the blue and orange circles denote images of two individual turtles. If two images are connected with edges, these images are matched, i.e. the method predicts that they contain the same individual. For instance, the four images of the “blue” turtle in the query set are connected with the “blue” turtle in the reference set and, therefore, are correctly predicted, similarly for the two images of the “orange” turtle. There are four “orange” turtles for which no prediction is made since they are not connected to the reference set.

By exploiting photographs of the same individual with various head orientations, this graph structure allows matching left and right head profiles, which otherwise would be impossible due to these patterns always being different. We provide an example in Fig. 6, depicting various poses of the same turtle. While there is no overlap of scales on the leftmost and rightmost photographs, these are nevertheless matched via the intermediate poses. Interestingly in this example, the timestamps coincide for only one of the five matches.

We use *precision* and *recall* to evaluate the performance

of this method. Precision is defined as the ratio of the number of correct predictions over all predictions, and recall is defined as the ratio of correct predictions over the size of the query set. In the example of Fig. 5, precision is 100% since all predictions are correct. However, since only six out of ten turtles in the query set are (correctly) predicted, recall is only 60%.

3.2. Neural network-based method

Neural network-based methods approach the re-identification task from a different viewpoint. Instead of making pairwise comparisons, they train a classifier on the whole reference set. Moreover, instead of creating a graph and making predictions for multiple images at once, they use the trained classifier to make predictions for each image from the query set separately. As neural networks make a prediction for all samples from the query set, precision and recall coincide. These terms are commonly known as *accuracy*. We refer again to the supplementary material for a specific description of the network we use.

3.3. Closed- and open-set problems

The *closed-set problem* refers to the case where the reference and the query sets contain the same individuals [39]. It assumes that the focal population never changes which is not realistic since new individuals are added (new recruits) and removed (migrations or death) over time. Therefore, it is natural to consider the situation where individuals are present in the query set but not in the reference set or vice versa. This is known as the *open-set problem* [39]. The open-set problem is common for wildlife dataset curators. This is because, at any given time, they obtain new images (e.g. from the current year) typically containing both old and new individuals, and they aim to match them to a

database consisting of all the images obtained before that time point (e.g. previous years).

3.4. Splits into reference and query sets

As described previously, the standard way to evaluate a re-identification algorithm is to split the evaluating dataset into a reference and a query set and verify its performance on the latter. We describe three possible such splits:

- **random (time-unaware) split:** the split of the dataset is done randomly without taking timestamps into account. It results in a *closed-set problem* whenever it is performed in a stratified setting (splitting the images of each individual separately).
- **time-proportion split:** the dataset is split based on time. The days that each individual was photographed are sorted in chronological order, and a fixed proportion (usually one half) of them is assigned to the reference set, with the rest assigned to the query set. Therefore, images of an individual taken on the same day belong to only one of these subsets. Individuals photographed only in one day are ignored for this split. This split always results in a *closed-set problem* since images of every individual are both in the reference and the query set.
- **time-cutoff split:** this split is similar to the previous case, but it is based on a cutoff time point rather than a fixed proportion of days. The reference set contains all photographs before the cutoff date, while the query set all photographs after the cutoff date. It usually results in an *open-set problem* since it is natural to have individuals appearing only after the cutoff date.

The open-set problem is much closer to the real-world re-identification settings than the closed-set problem. Therefore, the time-cutoff split should be preferred for method evaluation. When the closed-set problem is chosen for evaluation due to its simplicity, then the time-proportion split should be preferred over the random split. This is because the latter contains very similar images (photographs taken within seconds or consecutive video frames) in the reference and the query set, making it relatively simple for an algorithm to match them.

4. Results

This section evaluates the bias introduced by ignoring timestamps. We compare the time-aware (time-proportion or time-cutoff) with the random (time-unaware) split. For a fair comparison, the number of images of each individual in the reference set for the random split is set to be the same as in the time-aware split. Every experiment was performed on the bounding boxes containing the heads. Since the neural network always predicts an individual and the feature-based

method may give no prediction, we use different evaluation metrics for the two methods. Therefore, we provide no comparison between the feature-based method and neural networks.

4.1. Closed-set problem

For the closed-set problem, we investigate the time-proportion and the random splits. This results in a reference set with 3168 images and a query set with 3337 images for both splits. Tab. 4 lists the performance of both methods and splits. We observe that for both methods, the measured metric drops approximately to one half when the time-proportion split is used. For example, the recall for the feature-based method drops from 53.7% for the random split to 23.4% for the time-proportion split, meaning that the former overestimates the performance of the method by more than 100%. This is connected to the fact that the number of correct predictions drops from 1792 to 781, and the number of no-predictions increases from 1544 to 2554. The performance of the neural network exhibits similar drops, with an accuracy drop from 83.2% to 47.6%. Furthermore, the feature-based method has high precision, providing almost no wrong predictions; only one out of 1793 predictions was wrong for the random split.

4.2. Open-set problem

For the open-set problem, we focus on a comparison between the time-cutoff and random splits. The time-cutoff split considers the query set as one year (such as 2016) and the reference set the previous years (such as 2010–2015). Since the dataset spans 12 years, this gives rise to 11 time-cutoff splits. These splits naturally correspond to real-world splits when the curator matches newly obtained images of one year to images known from the previous years. We present the cumulative results in Tab. 5. As in the closed-set problem, we observe that the time-cutoff split leads to significantly worse performance. Since we solve the open-set problem, all individuals without a prediction are considered newly recruited individuals. While the number of correct predictions for new individuals is approximately the same for the time-cutoff and random splits, the latter results in a significantly lower number of wrong predictions, indicating again an overestimation of the method’s performance. Since neural networks require certain modifications to deal with the open-set setting, we consider only the feature-based method.

4.3. Transferability of results

Tab. 6 and Tab. 7 demonstrate transferability of results. We use the same settings as in Sec. 4.1. The former table shows experiments on SeaTurtleID with different backbones, while the latter table shows the results on different datasets with the best-performing Swin-B/p4w7 backbone.

split	feature-based method					neural network		
	prediction given		no prediction	metrics		prediction given		metric
	correct	wrong		precision	recall	correct	wrong	accuracy
time-proportion	781	2	2554	99.7%	23.4%	1588	1749	47.6%
random	1792	1	1544	99.9%	53.7%	2776	561	83.2%

Table 4: Comparison of the time-aware (time-proportion) and random (time-unaware) splits for the closed-set problem.

split	prediction given		new individual		metrics	
	correct	wrong	correct	wrong	precision	recall
time-cutoff	638	10	3800	3053	98.5%	17.3%
random	1973	7	3800	1721	99.6%	53.4%

Table 5: Comparison of the time-aware (time-cutoff) and random (time-unaware) splits for the open-set problem.

backbone	time-proportion	random
ResNeXt-50	38.6%	63.4%
EfficientNet-B0	39.9%	76.5%
ConvNeXt-B	47.2%	78.5%
ViT-Base/p32	45.2%	82.5%
Swin-B/p4w7	47.6%	83.2%

Table 6: Accuracy using different backbones.

	time-proportion	random
BelugaID	7.8%	12.1%
Cows2021	84.0%	79.9%
GiraffeZebraID	2.1%	30.1%
MacaqueFaces	91.1%	98.9%

Table 7: Accuracy using different datasets.

In all cases, the results on the random split are much better than on the time-aware split. The only exception is the Cows2021 dataset. However, this dataset spans only one month and the images are taken from a uniformly positioned camera, therefore, the timestamps are of little significance.

4.4. Further insights

Our results consistently show that whenever a time-aware split is applied, the performance of both methods drops significantly. We get further insight by considering all pairs of images of the same individuals with the same head orientation and see how their matching probability (proportion of correctly matched pairs) is affected by the time between them. Fig. 7 shows that the probability of the feature-based method to correctly match such image pairs strongly decreases as the time between them increases. For instance,

while this probability is 53.5% for images taken on the same day, it decreases to 2.5% for images taken more than one year apart.

We further interpret Fig. 7 with the specific example of turtle “t298”, which was observed only on two days: 01/07/2016 and 12/07/2020. The random split has images from both dates in both reference and query sets, while the time-proportion split contains all images from 2016 in the reference set and all images from 2020 in the query set. While there were 26 matches for 2016-2016 images and 140 matches for 2020-2020 images, there were only 2 matches for 2016-2020 images. This further implies that there are many matches between the reference and query sets for the random split but almost no such matches for the time-proportion split. Therefore, the random split unnaturally simplifies the real-world re-identification problem.

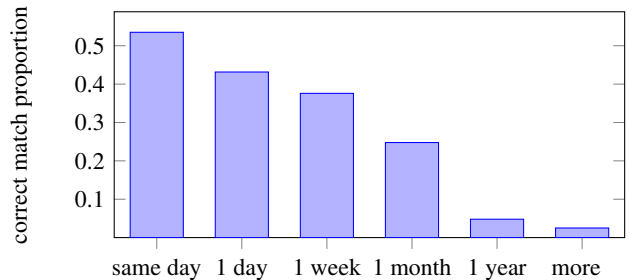


Figure 7: The probability of the feature-based method to correctly match pairs of images of the same individuals with the same head orientation (left side) decreases as the time between the two images increases.

5. Conclusions

We introduced *SeaTurtleID*, the longest-spanned publicly available wildlife photo-identification dataset. The dataset can be used for benchmarking re-identification algorithms but also for several other computer vision tasks. Based on the timestamp property of the dataset, we analysed the importance of including timestamps in datasets. We found them to be crucial and showed:

- Methods evaluated on datasets without timestamps lead to significant overestimation bias in performance.
- Timestamps allow to naturally perform more realistic splits into reference and query sets.

This further implies that datasets with timestamps are of a higher value than datasets without them. Hence, we recommend developers evaluate re-identification methods only on datasets with timestamps, using time-aware splits. At the same time, we urge wildlife dataset creators to include timestamps in their metadata.

References

- [1] Beluga ID 2022. <https://lila.science/datasets/beluga-id-2022>. Accessed: 10-09-2022. **2**
- [2] Turtle recall: Conservation challenge. <https://zindi.africa/competitions/turtle-recall-conservation-challenge>. Accessed: 10-09-2022. **2, 4**
- [3] Wildlife datasets. <https://github.com/WildlifeDatasets/wildlife-datasets>. Accessed: 02-03-2023. **2, 4**
- [4] Gwangbin Bae, Martin de La Gorce, Tadas Baltrušaitis, Charlie Hewitt, Dong Chen, Julien Valentin, Roberto Cipolla, and Jingjing Shen. Digiface-1M: 1 million digital face images for face recognition. In *Proceedings of the IEEE/CVF Winter Conference on Applications of Computer Vision (WACV)*, pages 3526–3535, 2023. **3**
- [5] Herbert Bay, Tinne Tuytelaars, and Luc Van Gool. SURF: Speeded up robust features. In *European Conference on Computer Vision*, pages 404–417. Springer, 2006. **5**
- [6] Drew Blount, Shane Gero, Jon Van Oast, Jason Parham, Colin Kingen, Ben Scheiner, Tanya Stere, Mark Fisher, Gianna Minton, Christin Khan, Violaine Dulau, Jaime Thompson, Olga Moskvyyak, Tanya Berger-Wolf, Charles V Stewart, Jason Holmberg, and J Jacob Levenson. Flukebook: an open-source AI platform for cetacean photo identification. *Mammalian Biology*, pages 1–19, 2022. **2**
- [7] Joakim Bruslund Haurum, Anastasija Karpova, Malte Pedersen, Stefan Hein Bengtson, and Thomas B Moeslund. Re-identification of zebrafish using metric learning. In *Proceedings of the IEEE/CVF Winter Conference on Applications of Computer Vision Workshops*, pages 1–11, 2020. **2**
- [8] Alexander Buslaev, Vladimir I. Iglovikov, Eugene Khvedchenya, Alex Parinov, Mikhail Druzhinin, and Alexandr A. Kalinin. Albumentations: Fast and Flexible Image Augmentations. *Information*, 11(2), 2020. **12**
- [9] Zhaowei Cai and Nuno Vasconcelos. Cascade R-CNN: Delying into high quality object detection. In *Proceedings of the IEEE Conference on Computer Vision and Pattern Recognition*, pages 6154–6162, 2018. **11**
- [10] Alice S Carpentier, Claire Jean, Mathieu Barret, Agathe Chassagneux, and Stéphane Ciccione. Stability of facial scale patterns on green sea turtles chelonia mydas over time: A validation for the use of a photo-identification method. *Journal of Experimental Marine Biology and Ecology*, 476:15–21, 2016. **3**
- [11] Steven JB Carter, Ian P Bell, Jessica J Miller, and Peter P Gash. Automated marine turtle photograph identification using artificial neural networks, with application to green turtles. *Journal of Experimental Marine Biology and Ecology*, 452:105–110, 2014. **5**
- [12] Kai Chen, Jiangmiao Pang, Jiaqi Wang, Yu Xiong, Xiaoxiao Li, Shuyang Sun, Wansen Feng, Ziwei Liu, Jianping Shi, Wanli Ouyang, Chen Change Loy, and Dahua Lin. Hybrid task cascade for instance segmentation. In *Proceedings of the IEEE/CVF Conference on Computer Vision and Pattern Recognition*, pages 4974–4983, 2019. **11**
- [13] Jonathan P Crall, Charles V Stewart, Tanya Y Berger-Wolf, Daniel I Rubenstein, and Siva R Sundaresan. Hotspotter-patterned species instance recognition. In *2013 IEEE Workshop on Applications of Computer Vision (WACV)*, pages 230–237. IEEE, 2013. **2, 5, 12**
- [14] Ekin D Cubuk, Barret Zoph, Jonathon Shlens, and Quoc V Le. RandAugment: Practical automated data augmentation with a reduced search space. In *Proceedings of the IEEE/CVF Conference on Computer Vision and Pattern Recognition Workshops*, pages 702–703, 2020. **12**
- [15] Jia Deng, Wei Dong, Richard Socher, Li-Jia Li, Kai Li, and Li Fei-Fei. Imagenet: A large-scale hierarchical image database. In *2009 IEEE Conference on Computer Vision and Pattern Recognition*, pages 248–255, 2009. **12**
- [16] Alexey Dosovitskiy, Lucas Beyer, Alexander Kolesnikov, Dirk Weissenborn, Xiaohua Zhai, Thomas Unterthiner, Mostafa Dehghani, Matthias Minderer, Georg Heigold, Sylvain Gelly, et al. An image is worth 16x16 words: Transformers for image recognition at scale. *arXiv preprint arXiv:2010.11929*, 2020. **12**
- [17] Stephen G Dunbar, Edward C Anger, Jason R Parham, Colin Kingen, Marsha K Wright, Christian T Hayes, Shahnaj Safi, Jason Holmberg, Lidia Salinas, and Dustin S Baumbach. Hotspotter: Using a computer-driven photo-id application to identify sea turtles. *Journal of Experimental Marine Biology and Ecology*, 535:151490, 2021. **2**
- [18] André C Ferreira, Liliana R Silva, Francesco Renna, Hanja B Brandl, Julien P Renoult, Damien R Farine, Rita Covas, and Claire Doutrelant. Deep learning-based methods for individual recognition in small birds. *Methods in Ecology and Evolution*, 11(9):1072–1085, 2020. **2**
- [19] Jing Gao, Tilo Burghardt, William Andrew, Andrew W Dowsey, and Neill W Campbell. Towards self-supervision for video identification of individual holstein-friesian cattle: The cows2021 dataset. *arXiv preprint arXiv:2105.01938*, 2021. **2**

- [20] Kaiming He, Xiangyu Zhang, Shaoqing Ren, and Jian Sun. Deep residual learning for image recognition. In *Proceedings of the IEEE Conference on Computer Vision and Pattern Recognition*, pages 770–778, 2016. 11
- [21] Jason Holmberg, Bradley Norman, and Zaven Arzoumanian. Estimating population size, structure, and residency time for whale sharks rhinodon typus through collaborative photo-identification. *Endangered Species Research*, 7(1):39–53, 2009. 2
- [22] Matthias Korschens and Joachim Denzler. ELPephants: A fine-grained dataset for elephant re-identification. In *Proceedings of the IEEE/CVF International Conference on Computer Vision Workshops*, pages 0–0, 2019. 2
- [23] Gary B. Huang Erik Learned-Miller. Labeled faces in the wild: Updates and new reporting procedures. Technical Report UM-CS-2014-003, University of Massachusetts, Amherst, May 2014. 3
- [24] Shuyuan Li, Jianguo Li, Hanlin Tang, Rui Qian, and Weiyao Lin. Atrw: A benchmark for amur tiger re-identification in the wild. In *Proceedings of the 28th ACM International Conference on Multimedia*, MM '20, pages 2590–2598, 2020. 2
- [25] Ze Liu, Yutong Lin, Yue Cao, Han Hu, Yixuan Wei, Zheng Zhang, Stephen Lin, and Baining Guo. Swin transformer: Hierarchical vision transformer using shifted windows. In *Proceedings of the IEEE/CVF International Conference on Computer Vision*, pages 10012–10022, 2021. 11, 12
- [26] Zhuang Liu, Hanzi Mao, Chao-Yuan Wu, Christoph Feichtenhofer, Trevor Darrell, and Saining Xie. A convnet for the 2020s. In *Proceedings of the IEEE/CVF Conference on Computer Vision and Pattern Recognition*, pages 11976–11986, 2022. 12
- [27] Ilya Loshchilov and Frank Hutter. Decoupled weight decay regularization. *arXiv preprint arXiv:1711.05101*, 2017. 12
- [28] David G Lowe. Distinctive image features from scale-invariant keypoints. *International Journal of Computer Vision*, 60(2):91–110, 2004. 5, 12
- [29] Dimitris Margaritoulis, Christopher J Dean, Gonçalo Lourenço, Alan F Rees, and Thomas E Riggall. Reproductive Longevity of Loggerhead Sea Turtles Nesting in Greece. *Chelonian Conservation and Biology*, 19(1):133–136, 2020. 3
- [30] Dimitris Margaritoulis and Aliki Panagopoulou. Greece. In P. Casale, editor, *Sea turtles in the Mediterranean: distribution, threats and conservation priorities*, pages 85–113. IUCN, 2010. 3
- [31] Oscar Moya, Pep-Luis Mansilla, Sergio Madrazo, Jose-Manuel Igual, Andreu Rotger, Antonio Romano, and Giacomo Tavecchia. APHIS: a new software for photo-matching in ecological studies. *Ecological Informatics*, 27:64–70, 2015. 2
- [32] Ekaterina Nepovinnikh, Tuomas Eerola, Vincent Biard, Piia Mutka, Marja Niemi, Mervi Kunnasranta, and Heikki Kälviäinen. SealID: Saimaa ringed seal re-identification dataset. *Sensors*, 22(19), 2022. 2
- [33] Kostas Papafitsoros, Lukáš Adam, and Gail Schofield. A social media-based framework for quantifying temporal changes to wildlife viewing intensity. *Ecological Modelling*, 2023. 2
- [34] Kostas Papafitsoros, Charalampos Dimitriadis, Antonios D Mazaris, and Gail Schofield. Photo-identification confirms polyandry in loggerhead sea turtles. *Marine Ecology*, 43(2):e12696, 2022. 2
- [35] Kostas Papafitsoros, Aliki Panagopoulou, and Gail Schofield. Social media reveals consistently disproportionate tourism pressure on a threatened marine vertebrate. *Animal Conservation*, 24(4):568–579, 2021. 1, 2, 3
- [36] Kostas Papafitsoros and Gail Schofield. Focal photograph surveys: Foraging resident male interactions and female interactions at fish-cleaning stations. In *Proceedings of the 36th Annual Symposium on Sea Turtle Biology and Conservation, Lima, Peru*, 2016. 2
- [37] Jason Remington Parham, Jonathan Crall, Charles Stewart, Tanya Berger-Wolf, and Daniel Rubenstein. Animal population censusing at scale with citizen science and photographic identification. In *2017 AAAI Spring Symposium Series*, 2017. 2
- [38] Ethan Rublee, Vincent Rabaud, Kurt Konolige, and Gary Bradski. ORB: An efficient alternative to SIFT or SURF. In *2011 International Conference on Computer Vision*, pages 2564–2571. IEEE, 2011. 5
- [39] Walter J Scheirer, Anderson de Rezende Rocha, Archana Sapkota, and Terrance E Boulton. Toward open set recognition. *IEEE Transactions on Pattern Analysis and Machine Intelligence*, 35(7):1757–1772, 2012. 6
- [40] Jonathan Schneider, Nihal Murali, Graham W Taylor, and Joel D Levine. Can *Drosophila melanogaster* tell who’s who? *PLoS ONE*, 13(10):e0205043, 2018. 2
- [41] Stefan Schneider, Graham W Taylor, Stefan Linquist, and Stefan C Kremer. Past, present and future approaches using computer vision for animal re-identification from camera trap data. *Methods in Ecology and Evolution*, 10(4):461–470, 2019. 1
- [42] Gail Schofield, Kostas A Katselidis, Panayotis Dimopoulos, and John D Pantis. Investigating the viability of photo-identification as an objective tool to study endangered sea turtle populations. *Journal of Experimental Marine Biology and Ecology*, 360(2):103–108, 2008. 3
- [43] Gail Schofield, Marcel Klaassen, Kostas Papafitsoros, Martin Lilley, Kostas A Katselidis, and Graeme C Hays. Long-term photo-id and satellite tracking reveal sex-biased survival linked to movements in an endangered species. *Ecology*, 11:e03027, 2020. 1, 2, 3
- [44] Gail Schofield, Kostas Papafitsoros, Chloe Chapman, Akanksha Shah, Lucy Westover, Liam CD Dickson, and Kostas A Katselidis. More aggressive sea turtles win fights over foraging resources independent of body size and years of presence. *Animal Behaviour*, 190:209–219, 2022. 1, 2, 3
- [45] Gail Schofield, Kostas Papafitsoros, Rebecca Haughey, and Kostas Katselidis. Aerial and underwater surveys reveal temporal variation in cleaning-station use by sea turtles at a temperate breeding area. *Marine Ecology Progress Series*, 575:153–164, 2017. 2
- [46] Alexandra Swanson, Margaret Kosmala, Chris Lintott, Robert Simpson, Arfon Smith, and Craig Packer. Snapshot Serengeti, high-frequency annotated camera trap images of

40 mammalian species in an African savanna. *Scientific data*, 2(1):1–14, 2015. 1

- [47] Mingxing Tan and Quoc Le. Efficientnet: Rethinking model scaling for convolutional neural networks. In *International Conference on Machine learning*, pages 6105–6114. PMLR, 2019. 12
- [48] Cameron Trotter, Georgia Atkinson, Matt Sharpe, Kirsten Richardson, A Stephen McGough, Nick Wright, Ben Burville, and Per Berggren. NDD20: A large-scale few-shot dolphin dataset for coarse and fine-grained categorisation. *arXiv preprint arXiv:2005.13359*, 2020. 2
- [49] Botswana Predator Conservation Trust. Panthera pardus csv custom export, 2022. 2
- [50] Maxime Vidal, Nathan Wolf, Beth Rosenberg, Bradley P Harris, and Alexander Mathis. Perspectives on individual animal identification from biology and computer vision. *Integrative and Comparative Biology*, 61(3):900–916, 2021. 1
- [51] Hendrik Weideman, Chuck Stewart, Jason Parham, Jason Holmberg, Kiirsten Flynn, John Calambokidis, D Barry Paul, Anka Bedetti, Michelle Henley, Frank Pope, and Jerenimo Lepirei. Extracting identifying contours for African elephants and humpback whales using a learned appearance model. In *Proceedings of the IEEE/CVF Winter Conference on Applications of Computer Vision*, pages 1276–1285, 2020. 2
- [52] Ross Wightman. PyTorch Image Models. <https://github.com/rwightman/pytorch-image-models>, 2019. 12
- [53] Claire L Witham. Automated face recognition of rhesus macaques. *Journal of Neuroscience Methods*, 300:157–165, 2018. 2
- [54] Saining Xie, Ross Girshick, Piotr Dollár, Zhuowen Tu, and Kaiming He. Aggregated residual transformations for deep neural networks. In *Proceedings of the IEEE conference on computer vision and pattern recognition (CVPR)*, pages 1492–1500, Honolulu, 2017. 12
- [55] Silvia Zuffi, Angjoo Kanazawa, Tanya Berger-Wolf, and Michael J Black. Three-D safari: Learning to estimate zebra pose, shape, and texture from images ”in the wild”. In *Proceedings of the IEEE/CVF International Conference on Computer Vision*, pages 5359–5368, 2019. 2

A. Additional supporting figures about the SeaTurtleID dataset

Fig. S2 shows a sample of original images from the SeaTurtleID dataset², highlighting the variety of photographs (poses, orientations, backgrounds etc).

Fig. S3 displays photographs of seven individuals (one individual per row) showing the variability of the unique facial scale patterns of loggerhead sea turtles. The scales on the left and right sides of the head are different in a given individual, making it impossible to match them without any intermediate images.

²We refer to www.kaggle.com/wildlifedatasets/SeaTurtleID for better quality photographs.

Fig. S4 shows further examples of different visual appearances of the same individual sea turtles over long periods of time due to different factors like camera capture conditions and animal ageing. The shapes of the facial scales remained stable, but other features have changed over time, like colouration, pigmentation, shape, and scratches.

B. Time-aware vs random (time-unaware) splits for a specific individual turtle

In Section 4.3 we highlighted the difference between a time-aware and a random split for the specific turtle “t298”. We recall that this turtle was observed only once in 2016 and once in 2020, and there were 26 matches for 2016-2016 images, 140 matches for 2020-2020 images and only 2 matches for 2016-2020 images.

We also recall that the second step of the feature-based method creates a graph which is the basis for making predictions for the images in the query set. In this particular case, this graph consisted of two connected components for the left and right sides of the turtle head, respectively. We focus here only on the components of the right side. Fig. S5 shows the time-aware split.³ Here, the reference set images are from 2016, while the query set images are from 2020. As we mentioned in the main text, there is a significant difference in image colouration as the 2020 images were captured with the use of flash, while the 2016 ones without. The clusters within the reference and cluster sets are very dense, meaning that it is easy to match images from the same day. On the other hand, there is only one match between the reference and query sets. However, this match allows us to correctly classify all images from the query set. Without this match, all images from the query set would be without any prediction. Fig. S6 shows the same situation for the random split, where we randomly shuffled the images into the reference and query sets. While there is the same number of matches as in Fig. S5, there are now 21 matches between the reference and query sets instead of only 1. This creates much robust clusters where even by removing several edges (matches), the predictions would not be affected. This further indicates why the time-aware split is much more challenging than the random one, yet more realistic with respect to the real-world re-identification tasks.

C. Detailed description of methods

A basic description of the methods used is provided in the main text. Here, we provide additional details.

Turtle head segmentation For the turtle head segmentation, we employed backbones Hybrid task cascade [12] and Swin transformer [25] with detection architectures Cascade mask R-CNN [9] and ResNet-50 [20]. Combining these

³It is possible to zoom in the pdf file to see the head details.

two backbones and two detection architectures results in the four models mentioned in the main text. Both backbones were initialised with weights obtained from pre-training on the ImageNet dataset [15]. For the dataset augmentation, we used random flip. All models were trained for 12 epochs. Models with the ResNet-50 backbone were trained with the stochastic gradient descent with learning rate 0.2, momentum 0.9 and weight decay 0.0001. Models with the Swin transformer backbone were trained with AdamW [27] with learning rate 0.0001 and weight decay 0.05.

Description of the feature-based method The first step of the feature-based method extracts SIFT features [28] from all images. Then for each pair of images, it matches feature vectors from both images based on their similarity; we denote the similarity between images i and j by s_{ij} . The usual way to make a prediction for an image i is to find $\arg \max_j s_{ij}$, i.e., an image with the largest similarity between feature vectors, see HotSpotter [13]. Here we adopt an alternative approach by finding a projective transform between the set of ten feature vectors with the largest similarity. Such transform is generated by a 3×3 matrix T , whose 2×2 leftmost submatrix \tilde{T} is the rotation matrix. We accept that the two images contain the same individual if the projective transform is “nice”, namely if the condition number of T is less than 100000 and the condition number of \tilde{T} is less than 100. The advantage of this approach is that, in addition to the feature similarity, also the relative spatial position of the features is taken into account by rejecting matches that are based on features that have high similarity but are located in different positions of the turtle’s head, see Fig. S1.

We used a classifier with the Swin-B/p4w7 architecture [47]. We adjusted the number of classes to match the number of individuals in the training dataset, initialised the model with weights obtained from pre-training on the ImageNet-1k dataset [15] and fine-tuned the weights on our training dataset. We trained the model for 100 epochs with batch size 128 and the Adam optimiser with a learning rate of 0.001. During training, each image was randomly cropped and resized to 224×224 pixels. Additionally, we normalised each channel using channel means and standard deviations. To compensate for a lower number of samples in our training dataset, we used RandAugment [14] data augmentation.

Description of neural networks We employed a variety of well-known CNN- and transformer-based architectures, i.e., ResNeXt-50 [54], EfficientNet-B0 [47], ConvNeXt-B [26], ViT-Base/32 [16], and Swin-B [25]. We also compared performance of the best model (Swin-B) on the animal re-identification datasets BelugaID, Cows2021, GiraffeZebraID, and MacaqueFaces. All neural network architectures were initialized from publicly available ImageNet-

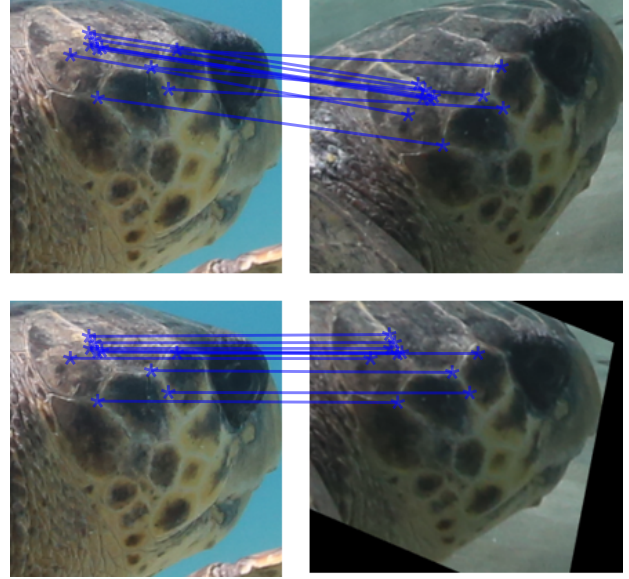


Figure S1: The top row shows the matching of two photographs via connecting SIFT features. The bottom row shows the same matching after applying a projective transform to the right image. The head positions overlap after the application of the projective transform and the parallel alignment of the features indicates that they have the same relative spatial position. This approach makes the matching more robust and less prone to errors.

1k pre-trained checkpoints [52] and further fine-tuned for 100 epochs. Mini-batch gradients were accumulated to reach an effective size of 128 for all the architectures – 4 batches of size 32. SGD with momentum (0.9) was used as an optimizer with a standard cosine learning rate (LR) annealing. The loss was calculated as softmax cross-entropy. While training, we employed the Random Resized Crop (with scale of 0.8–1.0) and the Random Augment [14] (with magnitude 20) data augmentation techniques from the Albumentations library [8]. All images were resized to match the pre-trained model input size of 224×224 , re-scaled from 0–255 to 0–1 and standardized by mean 0.5 and standard deviation 0.5 values in each channel.

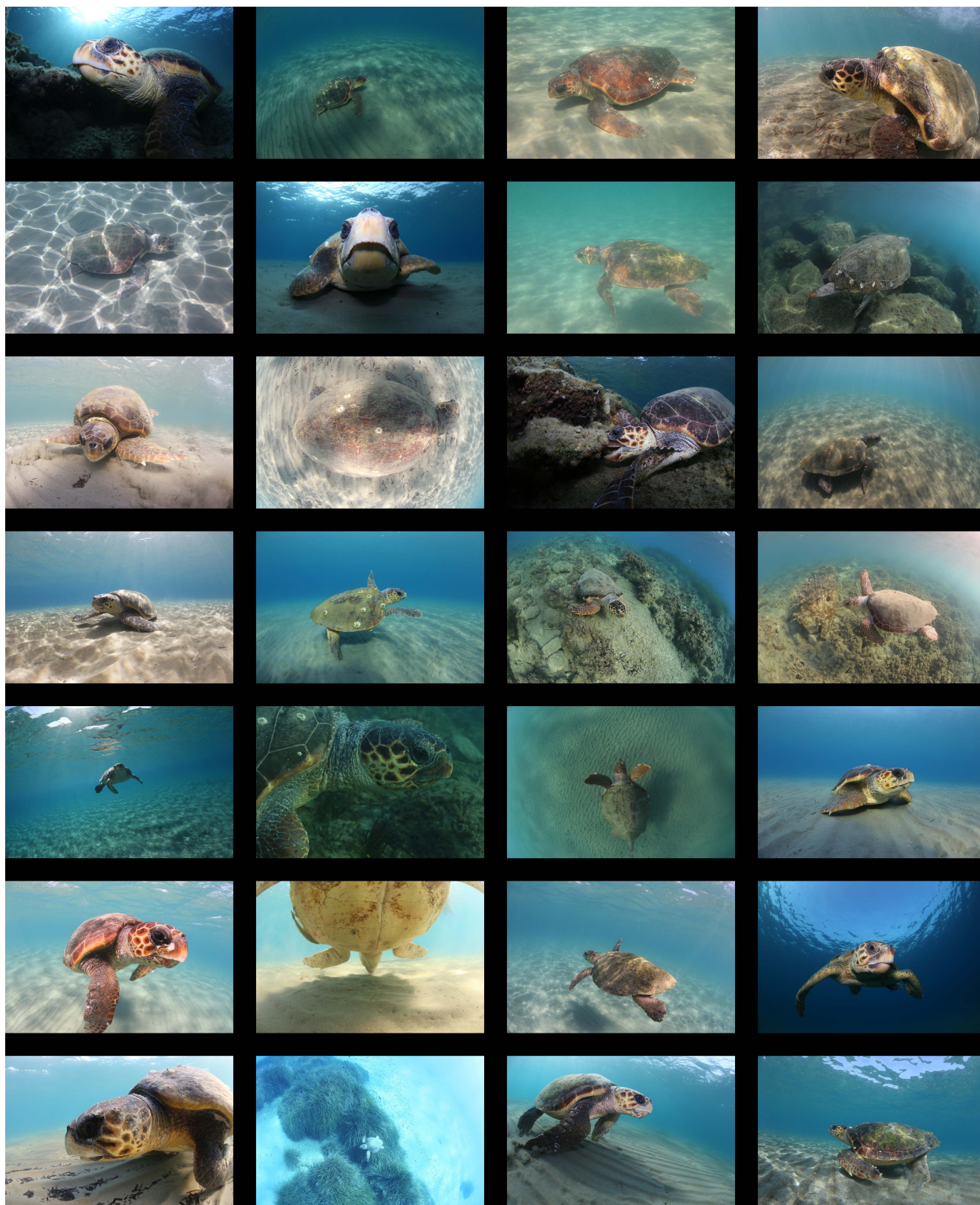


Figure S2: Examples of original photographs from the SeaTurtleID dataset.

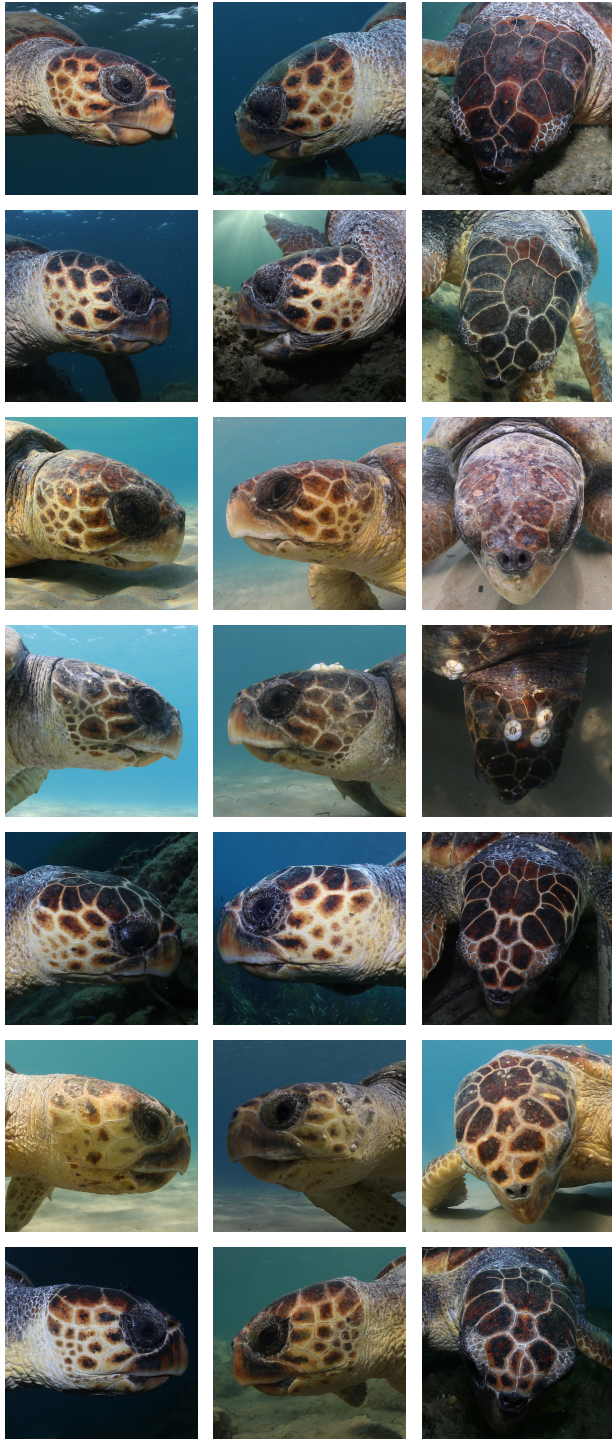


Figure S3: Examples of 7 individuals (one individual per row) that show the variability of unique facial scale patterns of loggerhead sea turtles. From left to right: right lateral facial scales, left lateral facial scales, dorsal head scales.

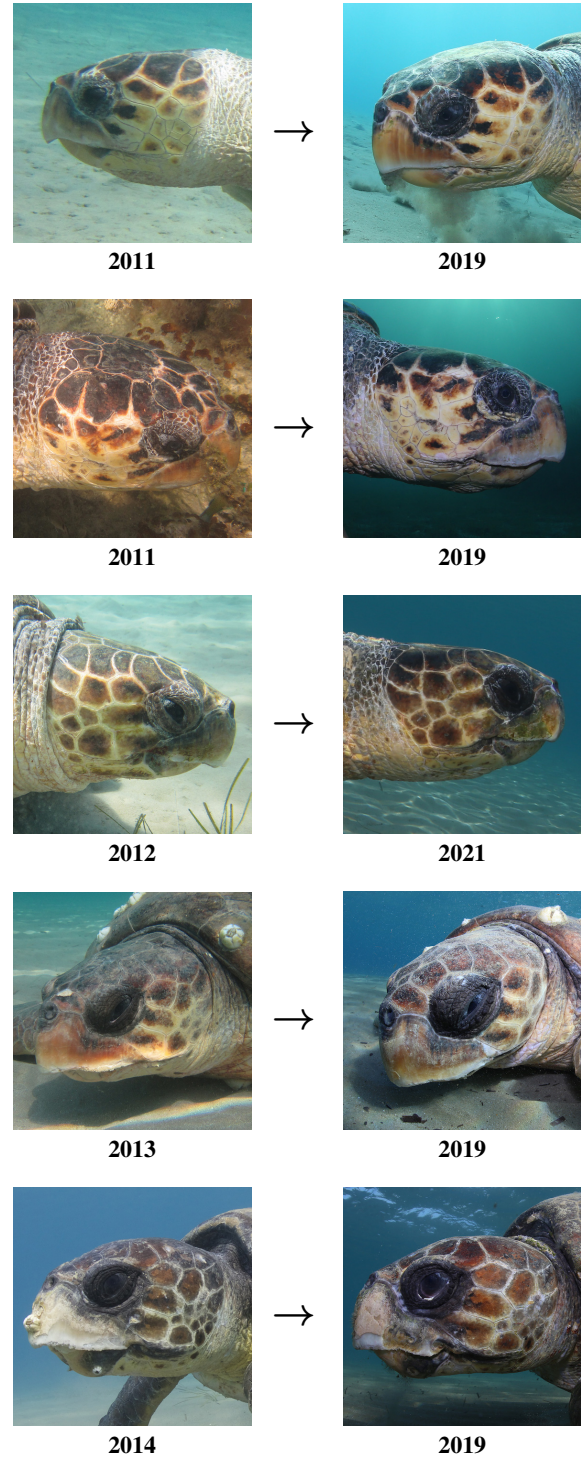


Figure S4: Further examples of different visual appearances of the same individual sea turtles over long periods of time due to different factors like camera capture conditions and animal ageing. The shapes of the facial scales remained stable, but other features have changed over time, like colouration, pigmentation, shape, and scratches.

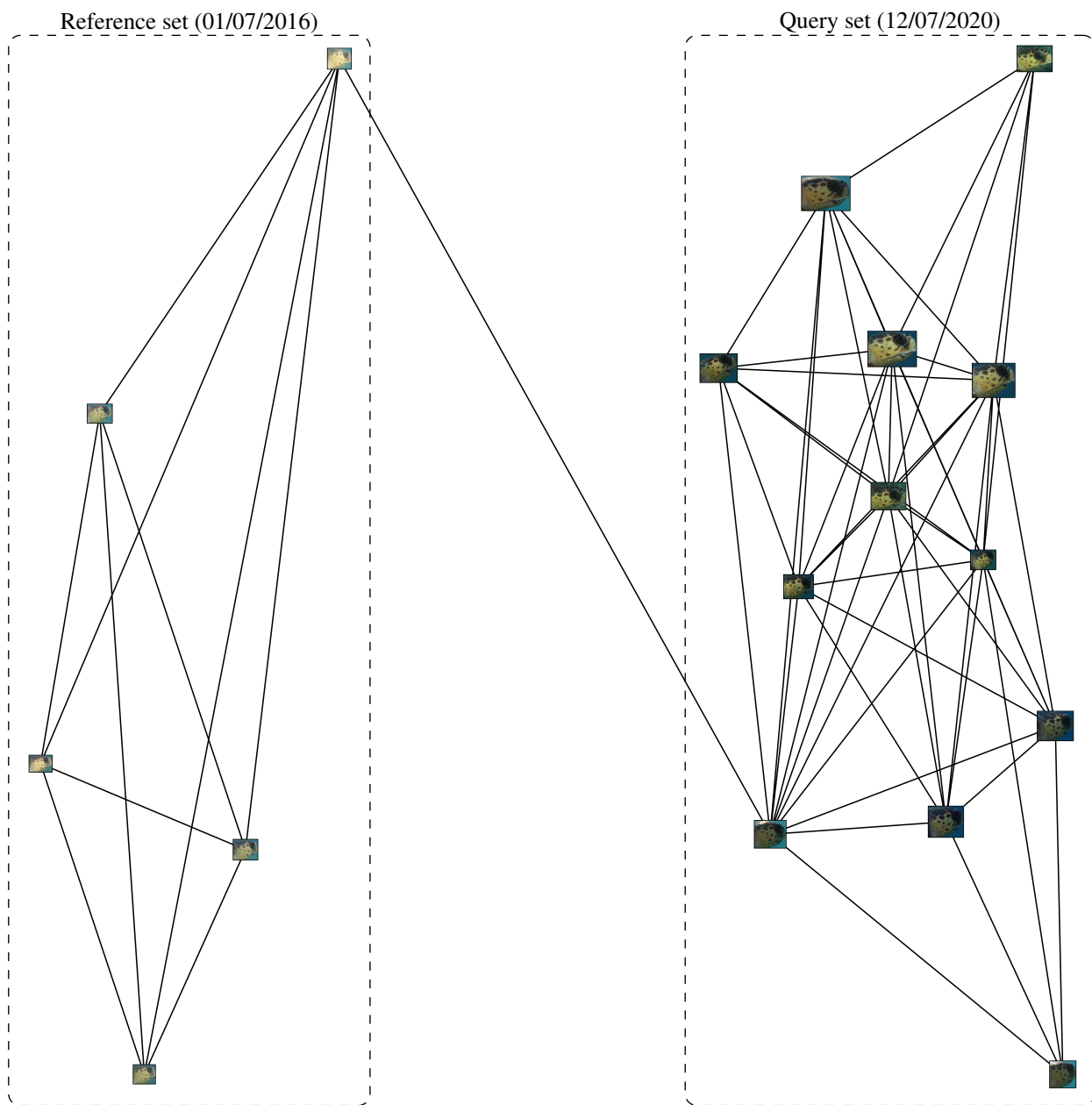


Figure S5: The matches between the reference and query sets for the time-aware split, for the individual turtle "t298": While all images in the query set are correctly classified, removing the single correct match between the reference and query set would lead to no prediction.

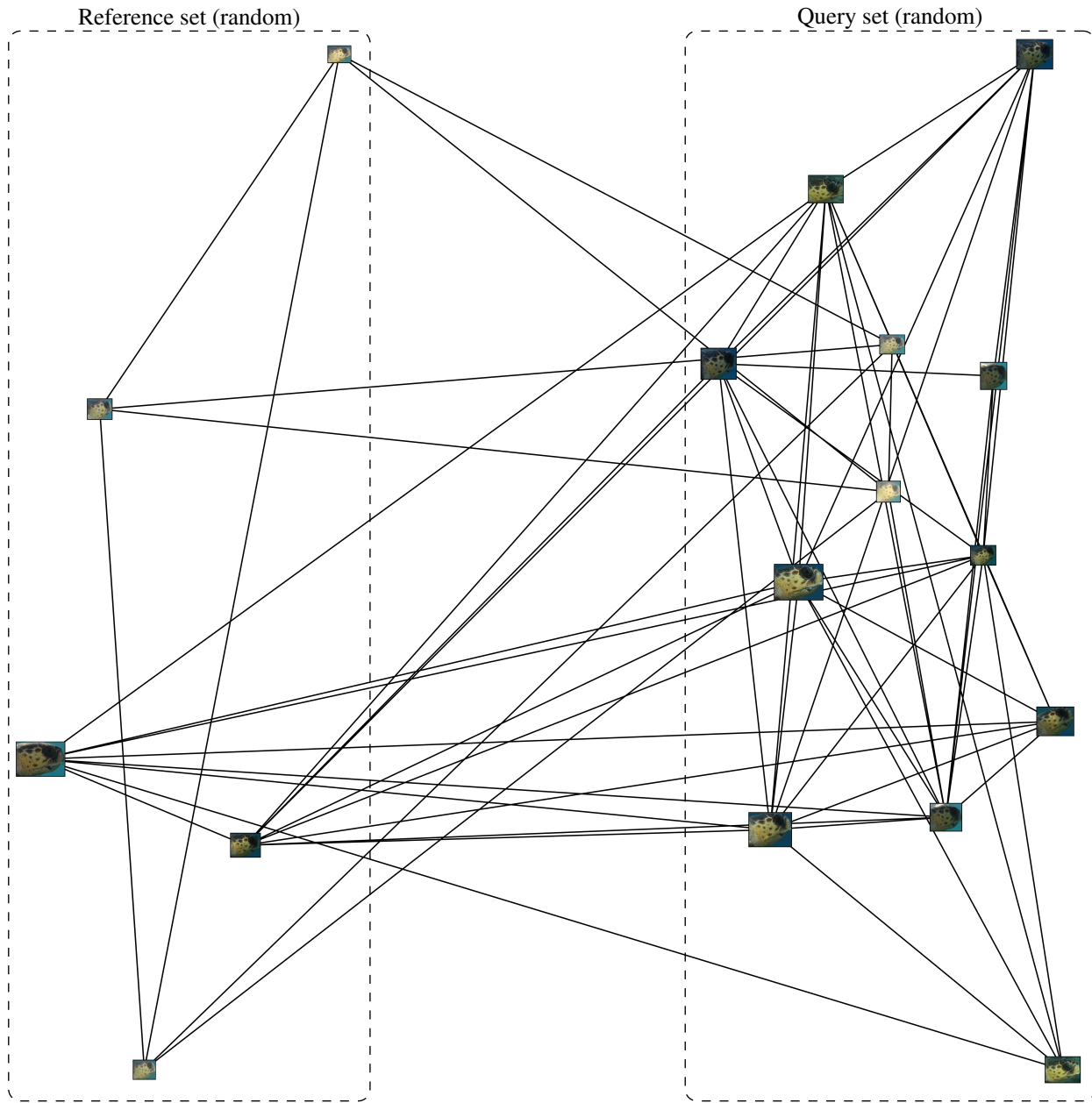


Figure S6: The matches between the reference and query set for the random split, for the individual turtle “t298”: The clustering is robust, meaning that by removing a small number of edges (matches), no prediction would be affected. Comparing this with Fig. S5 implies that the random split is much less challenging than the time-aware split, but it does not correspond to real-world re-identification tasks.